Lattice site investigation of F in preamorphized Si

F. Bernardi, J. H. R. dos Santos, and M. Behar
Instituto de Física da Universidade Federal do Rio Grande do Sul, Avenida Bento Gonçalves 9500, C. P. 15051, 91501-970, Porto Alegre, RS, Brazil

A. Kling
Instituto Tecnológico e Nuclear, Estrada Nacional 10, 2686-953 Sacavém, Portugal and Centro de Física Nuclear da Universidade de Lisboa, 1649-003, Lisbon P-2685, Portugal

(Received 29 January 2007; revised manuscript received 16 April 2007; published 5 July 2007)

The lattice location of F atoms in Si was experimentally studied. Si single crystals were amorphized, implanted with F, and afterwards the amorphous layer was recrystallized. Some of the samples prepared in this way were also annealed at 750 °C for 60 min. The $^{19}F(p,\alpha\gamma)^{16}O$ resonant nuclear reaction at 340.5 keV was employed to measure the probability of a close encounter between protons and F nuclei as a function of the incident angle with respect to six major crystalline directions. The predictions of several *ab initio* calculations proved to be incompatible with the present experimental findings.

DOI: 10.1103/PhysRevB.76.033201 PACS number(s): 61.72.Tt, 66.30.Jt

The miniaturization of complementary metal-oxide-semiconductor (CMOS) devices requires the confinement of dopants very close to the surface. In the microelectronics industry, the dopants are introduced through ion implantation. This technique is widely used because the depth and concentration of the dopant are easily controlled and reproduced. However, the implantation process generates point defects (self-interstitials and vacancies) in the target at a concentration well above the thermodynamical equilibrium level.[1] These defects undesirably accelerate the dopant diffusion. This phenomenon is called transient-enhanced diffusion (TED), and it may be several orders of magnitude faster than normal thermal diffusion. TED is particularly dramatic for boron,[2] the most frequently used *p* dopant, hindering thus the further miniaturization of CMOS devices.

In order to reduce the boron TED, coimplantation of F is currently used in the microelectronics industry, although the role F plays in the reduction of boron TED has not yet been entirely understood. To better understand the mechanism whereby F leads to a decrease of boron TED, substantial experimental and theoretical work has been carried out. Up to now, it is known that the slowing down of boron TED occurs by the interaction between F and point defects, and it has been suggested that F atoms form complexes with these defects.[3–9]

By *ab initio* calculations, several authors[5,7,8,10] have found that the lowest-energy state for a single interstitial F in Si is at the bond-centered the (BC) site in the +1 charge state or at the tetrahedral (T) site in the −1 charge state, depending on the Fermi energy. However, in Refs. 5 and 7 it was obtained that fluorine-vacancy (FV) complexes are highly favored over the interstitial configuration. From the experimental standpoint, the detection of FV complexes by positron annihilation spectroscopy has been reported in Refs. 3, 4, and 9 and also through sheet resistance measurement in Ref. 6. On the other hand, electric quadrupole hyperfine interaction and preliminary channeling experiments have indicated that F might occupy either bond or antibonding (AB) interstitial sites.[11,12]

In the present work, the lattice location of F atoms in Si was experimentally investigated. Czochralski *n*-type (P-doped) ⟨100⟩-Si single crystals with 10–20 Ω cm resistivity were amorphized from the surface down to a depth of about 440 nm with 200 keV 3×10^{15} Si^{+} cm^{-2} irradiation at liquid nitrogen temperature. Afterwards, the samples were implanted with 4×10^{14} F^{+} cm^{-2} at 80 keV. The Si irradiation was carried out at the 3-MV Tandetron accelerator of the Physics Institute of the Federal University of Rio Grande do Sul (IF-UFRGS) in a vacuum better than 10^{-6} mbar. The F implantation was performed at the 500-kV ion implanter of the same laboratory also in a vacuum better than 10^{-6} mbar. The F implantation energy was selected to place the F depth profile entirely within the amorphous region. Moreover, the implantation conditions were similar to those used in Ref. 13. After F implantation, the samples were recrystallized by solid-phase epitaxy (SPE) through annealing at 450 °C for 30 min plus 700 °C for 80 s in an N_2 ambient. The recrystallization of the amorphized layer was verified by Rutherford backscattering spectrometry (RBS) measurements under channeling conditions. Some of the samples prepared in this way were then annealed at 750 °C for 60 min in an N_2 ambient. The 750 °C/60 min annealing was performed in order to promote the interaction of F with self-interstitials released from the end-of-range region, as in Ref. 13. A subsequent site investigation should verify whether the interaction changes the F configuration.

The lattice location of F atoms in Si was then studied both post-SPE and post-SPE+annealing at 750 °C for 60 min. The close-encounter probability between protons and F nuclei was measured as a function of orientation around the axial directions ⟨100⟩, ⟨110⟩, ⟨111⟩, and ⟨211⟩ as well as across the planar directions {100} and {110}. The sample was placed on a three-axis goniometer with 0.005° precision in a chamber under a pressure less than 10^{-7} mbar, and the alignment of the crystal was performed using a 350-keV proton beam with a current of 10 nA and a divergence of about 0.03°. The backscattered protons were detected by a Si barrier detector with a resolution of 7 keV.

Next, the F angular scans were measured through the $^{19}F(p,\alpha\gamma)^{16}O$ resonant nuclear reaction at 340.5 keV with

1098-0121/2007/76(3)/033201(3) ©2007 The American Physical Society

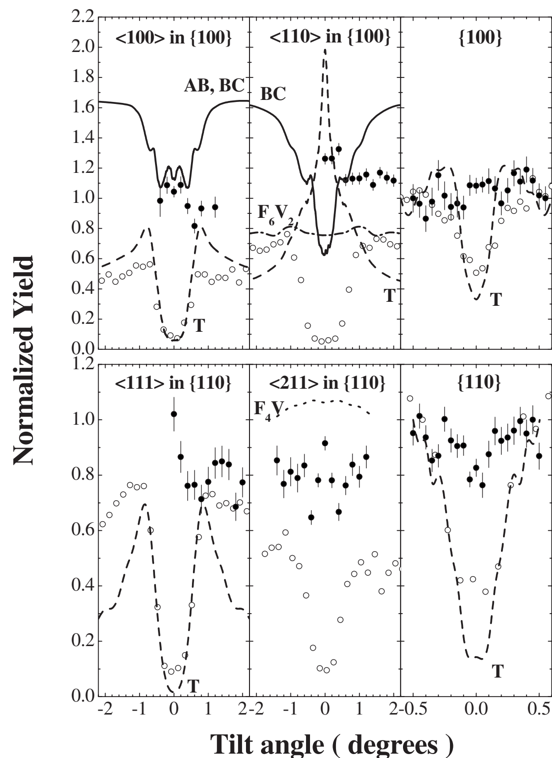

FIG. 1. Angular scans measured for the samples submitted to SPE+annealing at 750 °C for 60 min (●) shown together with the simulated curves for the BC (solid line), T (dashed line), and AB (solid line) interstitial sites, as well as for the F_4V (dotted line) and F_6V_2 (dash-dotted line) complexes. Si experimental angular scans (○) are also shown as reference.

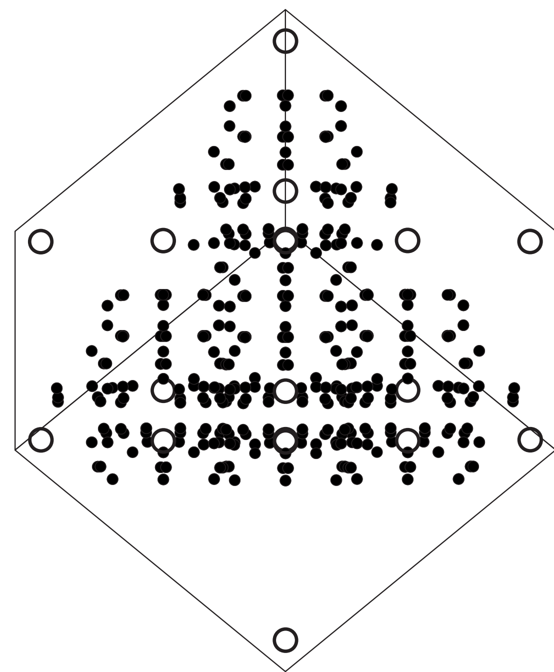

FIG. 2. Projection of the silicon unit cell (○) with the fluorine (•) symmetrically equivalent positions onto the plane perpendicular to the ⟨211⟩ axis, in the case of the F_4V complex.

natural width of (2.4±0.2) keV (Ref. 14) and cross section of about 162 mbarn (Ref. 15). For a given proton-beam fluence, the 6.4-MeV γ rays emitted by the ^{19}F nuclei were detected by a BGO [bismuth germanate ($Bi_4Ge_3O_{12}$)] scintillator as a function of the tilt angle between the beam and the crystal axis or plane. The axial scans were carried out along a plane of reference: namely, the plane {100} for the ⟨100⟩ and ⟨110⟩ axial scans and the plane {110} for the ⟨111⟩ and ⟨211⟩ axial scans. On the other hand, the planar scans were measured with the angle between the beam and the ⟨100⟩ axis fixed at 5°.

In the nuclear reaction analysis (NRA), the proton beam impinged onto the target at 350 keV. This energy was chosen so that the channeled proton beam can reach statistical equilibrium at the depth of the reaction[16] with the consequent flux peaking at the channel center. A proton beam with a typical current of the order of 0.5 μA was produced using the 500-kV ion implanter of the IF-UFRGS. In order to minimize beam-induced radiation damage, several measures were adopted. First, the value of the divergence was increased to about 0.08°. Second, each branch (going from zero degree until the largest tilt angle in absolute value) of every angular scan curve was always measured on a fresh spot of the target. Third, some scans were recorded in only one direction. Fourth, the points measured at tilt angles near zero were taken with a higher statistics, as they are more important to define the curve structure and result in less radiation damage. Furthermore, RBS spectra in the channeling condition recorded after angular scan measurements revealed no significant increase in the proton-backscattered minimum yield (χ_{min}) with respect to the initial condition. Finally, for each crystallographic direction, at least five independent F scans were performed, and the results were reproducible within the experimental errors.

In the attempt to reproduce the experimental angular distributions, the most probable sites were used as input in the computational code CASSIS (channeling adapted simulation of swift ions in solids).[17] It was assumed that the fluorine concentration was constant within the range where the nuclear reaction takes place, which is supported by a depth-profile measurement (not shown) performed through the same resonant nuclear reaction mentioned above. The one-dimensional thermal vibration amplitude of F was taken equal to the Si standard value of 0.07 Å.

Experimental RBS and NRA results for the angular yield scans of Si and F, respectively, are shown in Fig. 1 for the case of post-SPE samples+annealing at 750 °C for 60 min. After the 750 °C/60 min annealing, the shape of the angular distributions does not show any appreciable change with respect to the post-SPE case.

In Fig. 1, simulated curves are also displayed for the configurations most likely to be present in our experimental conditions,[18] which are, in decreasing order, the configurations F_6V_2, F_4V, and interstitial fluorine. The most stable interstitial locations for a single F atom in Si, according to theory[5,7,8,10] and previous experiments,[11,12] should be the BC, T, and AB sites. Yet it was not possible to fit the whole set of experimental yield curves with the AB, BC, and T sites, neither individually nor in a linear combination.

For the T site, F atoms should be hidden by the row of Si

atoms along the channels ⟨100⟩, ⟨111⟩, {100}, and {110}, being, therefore, in apparent incongruity with the experimental curves.

Regarding the simulations with F_nV_m $(n \geqslant 4, m \geqslant 1)$ complexes,[5,7] when one takes into account all the symmetry operations of the Si unit cell, there is a huge number of equivalent positions in the Si cell for each F atom of the complex, which is similar to a random dispersion of atoms. This situation can be clearly seen in Fig. 2, for projections of fluorine symmetrically equivalent positions onto the plane perpendicular to the ⟨211⟩ axis, in the case of the F_4V complex. Such a situation would produce an angular yield curve roughly constant (Fig. 1) around the respective axis, whereas the present experimental curves do show structures. The larger n, the larger the total number of F positions in the Si unit cell and the closer to constant all the simulated curves will be. Nonetheless, from the present experimental results, one cannot rule out the existence of other types of FV complexes than those discussed above.

In summary, the lattice location of F implanted into preamorphized Si has been studied both after recrystallization and after recrystallization plus annealing at 750 °C for 60 min. Channeling studies using the $^{19}F(p,\alpha\gamma)^{16}O$ resonant nuclear reaction for the detection of the F site have been performed for six crystallographic directions. The experimental angular yield curves are incompatible with bond-centered and tetrahedral sites, which were found by *ab initio* calculations to be the most likely interstitial sites for F atoms in Si. Furthermore, the presence at a detectable concentration of the F_nV_m $(n \geqslant 4, m \geqslant 1)$ clusters theoretically found in Refs. 5 and 7 is not consistent with the present experimental results. Finally, it seems that however F acts to decrease the boron TED in Si, its configuration does not change in the process.

The authors wish to acknowledge G. Impellizzeri, S. Mirabella, A. M. Piro, G. M. Lopez, and V. Fiorentini for numerous helpful discussions.

[1] J. F. Ziegler, J. P. Biersack, and U. Littmark, *The Stopping and Range of Ions in Solids*, 2nd ed. (Pergamon Press, New York, 1996).

[2] S. C. Jain, W. Schoenmaker, R. Lindsay, P. A. Stolk, S. Decoutere, M. Willander, and H. E. Maes, J. Appl. Phys. **91**, 8919 (2002).

[3] X. D. Pi, C. P. Burrows, and P. G. Coleman, Phys. Rev. Lett. **90**, 155901 (2003).

[4] P. J. Simpson, Z. Jenei, P. Asoka-Kumar, R. R. Robison, and M. E. Law, Appl. Phys. Lett. **85**, 1538 (2004).

[5] M. Diebel and S. T. Dunham, Phys. Rev. Lett. **93**, 245901 (2004).

[6] N. E. B. Cowern, B. Colombeau, J. Benson, J. Smith, W. Lerch, S. Paul, T. Graf, F. Cristiano, X. Hebras, and D. Bolze, Appl. Phys. Lett. **86**, 101905 (2005).

[7] G. M. Lopez, V. Fiorentini, G. Impellizzeri, S. Mirabella, and E. Napolitani, Phys. Rev. B **72**, 045219 (2005).

[8] S. A. Harrison, T. F. Edgar, and G. S. Hwang, Phys. Rev. B **74**, 121201(R) (2006).

[9] D. A. Abdulmalik, P. G. Coleman, N. E. B. Cowern, A. J. Smith, B. J. Sealy, W. Lerch, S. Paul, and F. Cristiano, Appl. Phys. Lett. **89**, 052114 (2006).

[10] A. Taguchi and Y. Hirayama, Solid State Commun. **116**, 595 (2000).

[11] K. B. Nielsen, H. K. Schou, T. Lauritsen, G. Weyer, I. Stensgaard, J. W. Petersen, and S. Damgaard, J. Phys. C **17**, 3519 (1984).

[12] D. Surono, F.-J. Hambsch, and P. W. Martin, Hyperfine Interact. **96**, 23 (1995).

[13] G. Impellizzeri, J. H. R. dos Santos, S. Mirabella, F. Priolo, E. Napolitani, and A. Carnera, Appl. Phys. Lett. **84**, 1862 (2004).

[14] D. Dieumegard, B. Maurel, and G. Amsel, Nucl. Instrum. Methods **168**, 93 (1980).

[15] J. R. Tesmer, M. Nastasi, J. C. Barbour, C. J. Maggiore, and J. W. Mayer, *Handbook of Ion Beam Analysis*, 1st ed. (Materials Research Society, Pittsburgh, 1995), p. 704.

[16] J. Lindhard, K. Dan. Vidensk. Selsk. Mat. Fys. Medd. **34**, 1 (1965).

[17] A. Kling, Nucl. Instrum. Methods Phys. Res. B **102**, 141 (1995).

[18] M. Diebel and S. T. Dunham, Phys. Rev. Lett. **96**, 039602 (2006).